Conduction channels of superconducting quantum point contacts

E. Scheer, J.C. Cuevas, A. Levy Yeyati, A. Martín-Rodero, P. Joyez, M.H. Devoret, D. Esteve and C. Urbina
[1] *Physikalisches Institut, Universität Karlsruhe, 76128 Karlsruhe, Germany;* [2] *Departamento de Física Teórica de la Materia Condensada C-V, Universidad Autónoma de Madrid, 28049 Madrid, Spain;* [3] *Service de Physique de l'Etat Condensé, Commissariat à l'Energie Atomique, Saclay, 91191 Gif-sur-Yvette Cedex, France*

Atomic quantum point contacts accommodate a small number of conduction channels. Their number N and transmission coefficients $\{T_{\rm n}\}$ can be determined by analyzing the subgap structure due to multiple Andreev reflections in the current-voltage (IV) characteristics in the superconducting state. With the help of mechanically controllable break-junctions we have produced Al contacts consisting of a small number of atoms. In the smallest stable contacts, usually three channels contribute to the transport. We show here that the channel ensemble $\{T_{\rm n}\}$ of few atom contacts remains unchanged up to temperatures and magnetic fields approaching the critical temperature and the critical field, respectively, giving experimental evidence for the prediction that the conduction channels are the same in the normal and in the superconducting state.

I. INTRODUCTION

An atomic size contact between two metallic electrodes can accommodate only a small number of conduction channels. The contact is thus fully described by a set $\{T_{\rm n}\} = \{T_1, T_2, ...T_{\rm N}\}$ of transmission coefficients which depends both on the chemical properties of the atoms forming the contact and on their geometrical arrangement. Experimentally, contacts consisting of even a single atom have been obtained using both scanning tunneling microscope and break-junction techniques [1]. The total transmission $D = \sum_{n=1}^{N} T_{\rm n}$ of a contact is deduced from its conductance G measured in the normal state, using the Landauer formula $G = G_0 D$ where $G_0 = 2e^2/h$ is the conductance quantum [2].

Experiments on a large ensemble of metallic contacts have demonstrated the *statistical* tendency of atomic-size contacts to adopt configurations leading to some preferred values of conductance. The actual preferred values depend on the metal and on the experimental conditions. However, for many metals, and in particular 'simple' ones (like Na, Au...) which in bulk are good 'free electrons' metals, the smallest contacts have a conductance G close to G_0 [1,3–5]. Statistical examinations of Al point contacts at low temperatures yield preferred values of conductance at $G = 0.8\ G_0, 1.9\ G_0, 3.2\ G_0$ and $4.5\ G_0$ [6], indicating that single-atom contacts of Al have a typical conductance slightly below the conductance quantum. Does this mean that the single-atom contacts correspond to a single, highly transmitted channel ($T = 0.8$)? This question cannot be answered solely by conductance measurements which provide no information about the number or transmissions of the individual channels.

However, it has been shown that the *full* set $\{T_{\rm n}\}$ is amenable to measurement in the case of superconducting materials [7] by quantitative comparison of the measured current-voltage (IV characteristics) with the theory of multiple Andreev reflection (MAR) for a single channel BCS superconducting contact with arbitrary transmission T, developed by several groups for zero temperature $\Theta = 0$ and zero magnetic field $H = 0$ [8–11]. Although the typical conductance of single-atom contacts of Al ($G \simeq 0.8\ G_0$) is smaller than the maximum possible conductance for one channel, three channels with transmissions such that $T_1 + T_2 + T_3 \simeq 0.8$ have been found [7].

Moreover, there exist other physical properties which are not linear with respect to $\{T_{\rm n}\}$ as e.g. shot noise [16], conductance fluctuations [17], and thermopower [18], which also give information about the $\{T_{\rm n}\}$ of a contact. Although it is not possible to determine the full set of transmission coefficients with these properties, certain moments of the distribution and in particular the presence or absence of partially open channels can be detected. Recent experiments have shown that normal atomic contacts of Al with conductance close to G_0 contain incompletely open channels [16] in agreement with the findings in the superconducting state [7].

In previous work we have shown [13,14] how the conduction channels of metallic contacts can be constructed from the valence orbitals of the material under investigation. In the case of single-atom contacts the channels are determined by the valence orbitals of the central atom and its local environment. In particular for Al the channels arise from the contributions of the s and p valence bands. To the best of our knowledge it has never been observed in contacts of multivalent metals that a single channel arrives at its saturation value of $T = 1$ before at least a second one had opened. Single-atom contacts of the monovalent metal Au transmit one single channel with a transmission $0 < T \leq 1$ depending on the particular realization of the contact [14,15].

From the theoretical point of view no difference between the normal and superconducting states is expected, because (i) according to the BCS theory [19] the elec-

tronic wave functions themselves are not altered when entering the superconducting state, but only their occupation and (*ii*) MAR preserves electron-hole symmetry and therefore does not mix channels [20,21].

Experimental evidence for the equivalence of the normal and superconducting channels can be gained by tracing the evolution of the IV curves from the superconducting to the normal state in an external magnetic field and/or higher temperatures and comparing them to the recent calculations by Cuevas *et al.* of MAR in single channel contacts at finite temperatures [22] and including pair breaking due to magnetic impurities or magnetic field [23].

We show here that the channel ensemble $\{T_{\rm n}\}$ of few atom contacts remains unchanged when suppressing the superconducting transport properties gradually by raising the temperature or the magnetic field up to temperatures and magnetic fields approaching the critical temperature and the critical field, respectively. Although it is not possible to measure the full channel ensemble above the critical temperature or field, respectively, no abrupt change is to be expected since the phase transition (as a function of temperature) is of second order. Because the determination of the channel ensemble relies on the quantitative agreement between the theory and the experimental IVs, we concentrate here on the case of Al point contacts since we expect for this material the BCS theory to fully apply.

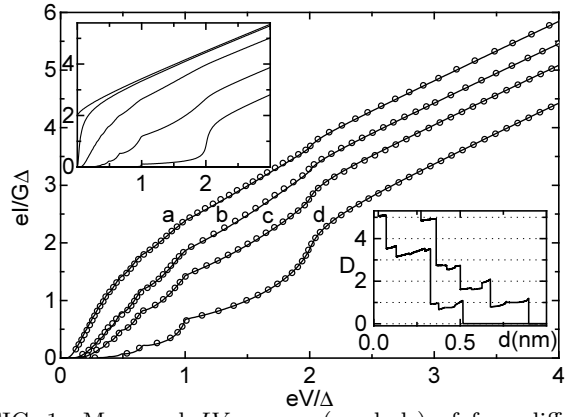

FIG. 1. Measured IV curves (symbols) of four different atomic contacts with $G \simeq 0.9\ G_0$ at $\Theta \leq 50$ mK and best numerical fits (lines). The $\{T_{\rm n}\}$ and total transmissions D obtained from the fits are: (a) $\{0.900, 0.108\}$, $D = 1.008$; (b) $\{0.802, 0.074\}$, $D = 0.876$; (c) $\{0.747, 0.168, 0.036\}$, $D = 0.951$; (d) $\{0.519, 0.253, 0.106\}$, $D = 0.878$. Current and voltage are in reduced units, the current axis is normalized with respect to the total conductance measured by the slope of the IV at high voltages $eV > 5\Delta$. Not all measured data points are shown. The measured gap was $\Delta/e = (184 \pm 2)\ \mu$V. Left inset: Theoretical IVs for a single channel superconducting contact for different values of T (from bottom to top: 0.1, 0.6, 0.9, 0.99, 1) after [10]. Right inset: typical total transmission traces measured as a function of the electrode distance d at $eV > 5\ \Delta$, while opening the contact at around 6 pm/s. The d axis has been calibrated by the exponential behavior in the tunnel regime.

II. TRANSPORT THROUGH A SUPERCONDUCTING QUANTUM POINT CONTACT

The upper left inset of Fig. 1 shows the theoretical IVs by Cuevas *et al.* [10] for zero temperature $\Theta = 0$ and zero field $H = 0$. A precise determination of the channel content of any superconducting contact is possible making use of the fact that the total current $I(V)$ results from the contributions of N independent channels:

$$I(V) = \sum_{n=1}^{N} i(V, T_n). \qquad (1)$$

This equation is valid as long as the scattering matrix whose eigenvalues are given by the transmission coefficients is unitary, i.e. the scattering is time independent. The $i(V,T)$ curves present a series of sharp current steps at voltage values $V = 2\Delta/me$, where m is a positive integer and Δ is the superconducting gap. Each one of these steps corresponds to a different microscopic process of charge transfer setting in. For example, the well-known non-linearity at $eV = 2\Delta$ arises when one electronic charge ($m = 1$) is transferred thus creating two quasiparticles. The energy eV delivered by the voltage source must be larger than the energy 2Δ needed to create the two excitations. The common phenomenon behind the other steps is multiple Andreev reflection (MAR) of quasiparticles between the two superconducting reservoirs [24,25]. The order $m = 2, 3, ...$, of a step corresponds to the number of electronic charges transferred in the underlying MAR process. Energy conservation imposes the threshold $meV \geq 2\Delta$ for each process. For low transmission, the contribution to the current arising from the process of order m scales as T^m. The contributions of all processes sum up to the so-called "excess current" the value of which can be determined by extrapolating the linear part of the IVs well above the gap $v > 5\Delta$ down to zero voltage. As the transmission of the channel rises from 0 to 1, the higher order processes grow stronger and the current increases progressively. The ensemble of steps is called "subharmonic gap structure", which was in fact discovered experimentally [26], has been extensively studied in superconducting weak links and tunnel junctions with a very large number of channels [27,28].

III. EXPERIMENTAL TECHNIQUES

In order to infer $\{T_{\rm n}\}$ from the IVs, very stable atomic-size contacts are required. For this purpose we have used micro-fabricated mechanically controllable break-

FIG. 2. Three point bending mechanism. The distance between the two counter-supports is 12 mm, and the substrate is 0.3 mm thick. The micrograph shows a suspended Al microbridge. The insulating polyimide layer was etched to free the bridge from the substrate. The third panel displays the wiring of the experimental setup.

junctions [29]. Our samples are 2 μm long, 200 nm thick suspended microbridges, with a 100 nm × 100 nm constriction in the middle (cf. Fig. 2). The bridge is broken at the constriction by controlled bending of the elastic substrate mounted on a three-point bending mechanism. A differential screw (100 μm pitch) driven by a dc-motor through a series of reduction gear boxes, controls the motion of the pushing rod that bends the substrate (Fig. 2).

The geometry of the bending mechanism is such that a 1 μm displacement of the rod results in a relative motion of the two anchor points of the bridge of around 0.2 nm. This was verified using the exponential dependence of the conductance on the interelectrode distance in the tunnel regime. This very strong dependence was used to calibrate the distance axis to an accuracy of about 20 %. The bending mechanism is anchored to the mixing chamber of a dilution refrigerator within a metallic box shielding microwave frequencies. The bridges are broken at low temperature and under cryogenic vacuum to avoid contamination.

The IV characteristics are measured by voltage biasing with $U = U_{\rm dc}$ the sample in series with a calibrated resistor $R_{\rm s} = 102.6\,{\rm k}\Omega$ and measuring the voltage drop across the sample (giving the V signal) and the voltage drop $V_{\rm S} = IR_{\rm s}$ across $R_{\rm s}$ (giving the I signal) via two low-noise differential preamplifiers. The differential conductance is measured by biasing with $U = U_{\rm dc} + U_1\cos(2\pi ft)$ using a lock-in technique at low frequency $f < 200$ Hz. All lines connecting the sample to the room temperature electronics are carefully filtered at microwaves frequencies by a combination of lossy shielded cables [30], and microfabricated cryogenic filters [31]. The cryostat is equipped with a superconducting solenoid allowing to control the field $\mu_0 H$ at the position of the sample within 0.05 mT. After having applied a magnetic field and before taking new $H = 0$ data we demagnetize carefully the solenoid. The temperature is monitored by a calibrated resistance thermometer thermally anchored to the shielding box. The absolute accuracy of the temperature measurement is about 5%.

IV. DETERMINATION OF THE CHANNEL TRANSMISSIONS

Pushing on the substrate leads to a controlled opening of the contact, while the sample is maintained at $\Theta < 100$ mK. As found in previous experiments at higher temperatures, the conductance G decreases in steps of the order of G_0, their exact sequence changing from opening to opening (see right inset of Fig. 1). The last conductance value before the contact breaks is usually between 0.5 and 1.5 G_0.

Figure 1 shows four examples of IVs obtained at $\Theta < 50$ mK on last plateaux of two different Al samples just before breaking the contact and entering the tunnel regime. The curves differ markedly eventhough they correspond to contacts having the same conductance of about $G \simeq 0.9\ G_0$ within 10%. The existence of IVs with the same conductance but different subgap structure implies the presence of more than one channel without further analysis. In particular, the examples shown here demonstrate that although they would correspond to the first maximum in the conductance histogram [6], they do not transmit a single channel, but at least two, with a variety of transmissions.

In Fig. 1 we also show the best least-square fits obtained using the numerical results of the $\Theta = 0$ theory of Cuevas *et al.* [10]. The fitting procedure decomposes the total current into the contributions of eight independent channels. Channels found with transmissions lower than 1% of the total transmission were neglected. When $N \leq 3$, this fitting procedure allows the determination of each $T_{\rm n}$ with an accuracy of 1% of the total transmission D. For contacts containing more channels only the 2 or 3 dominant channels (depending on their absolute value) can be extracted with that accuracy. Details of the fitting procedure are published in [7].

V. IVS OF AL POINT CONTACTS AT HIGHER TEMPERATURES

The right inset of Fig. 3 displays the evolution of the IV of contact (a) from Fig. 1 for three different temperatures below the critical temperature $\Theta_{\rm c} = 1.21\,{\rm K}$ (each trace is offset by 0.5 for clarity). When the temperature is increased the subgap structure is slightly smeared out due to the thermal activation of quasiparticles, and the position of the current steps is shifted to smaller voltages due to the reduction of the superconducting gap. Although the IVs are very smooth due to the dominance of an almost perfectly open channel, up to eight MAR processes are distinguishable in the ${\rm d}I/{\rm d}V$. The solid lines are calculated with the same set of transmissions $\{T_1 = 0.900, T_2 = 0.108\}$ for the temperatures indicated in the caption using the BCS dependence of the superconducting gap and the Fermi function for the respective temperature [22,25]. The quality of the fit does not vary with temperature.

In order to further interpret the data, we plot in Fig. 4 the theoretical zero temperature single channel ${\rm d}I/{\rm d}V$s for the same transmissions as in the inset in Fig. 1 in two different manners. In the left panel they are plotted as a function of eV/Δ showing the different shapes and

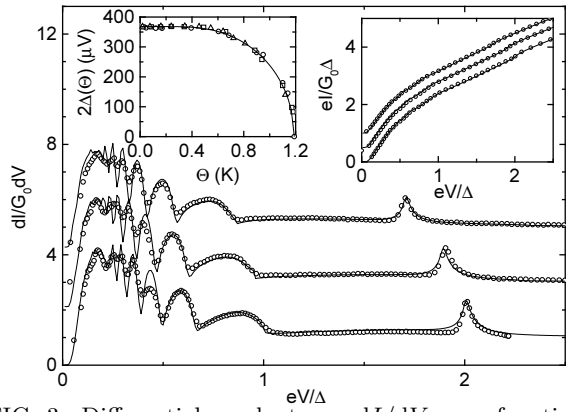

FIG. 3. Differential conductance $\mathrm{d}I/\mathrm{d}V$ as a function of voltage measured at $\Theta = 47$ mK (bottom), 640 mK (middle), and 810 mK (top) for a contact with total conductance $D = 1.008$. The two upper curves are offset by 2 each. The solid lines are fits using the same transmission ensemble $\{T_1 = 0.900, T_2 = 0.108\}$ for all three temperatures. Right inset: corresponding IVs offset by 0.5 each. Left inset: position of the $m = 1$ maximum in the $\mathrm{d}I/\mathrm{d}V$ curves. Data has been taken on three different contacts with G varying from 1 to 2 G_0. The line is the temperature dependence of the superconducting gap according to BCS theory for $\Delta(\Theta = 0) = 184\mu$V.

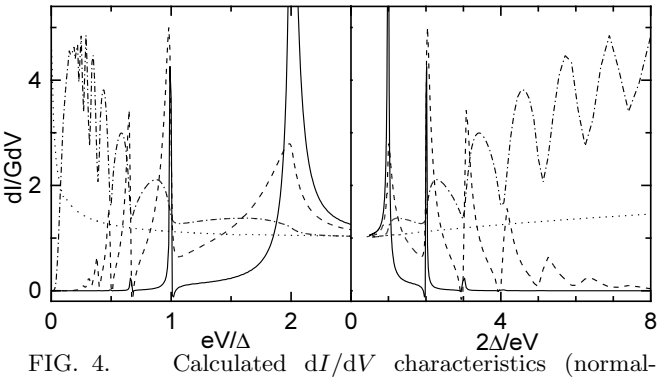

FIG. 4. Calculated $\mathrm{d}I/\mathrm{d}V$ characteristics (normalized to the conductance) of a single channel quantum point contact for transmission 0.1 (solid), 0.6 (dashed), 0.9 (dash-dotted), 1.0 (dotted) as a function of eV/Δ (left panel) and $m' = 2\Delta/eV$ (right panel). The maximum of the curve for $T = 0.1$ arrives at $12.6G$. The amplitude, the shape and the exact position of the individual maxima depend on the transmission. Only for small T the maxima are close to $V = 2\Delta/me$, for higher transmission they are shifted to lower voltages. The subgap structure is most pronounced for intermediate T.

amplitudes of the individual MAR processes for varying transmission. A small T gives rise to narrow conductance spikes, whereas a higher T yields round maxima at voltages $V < 2\Delta/me$ and pronounced minima close to the sub-multiple values $V = 2\Delta/me$. This behavior is clearly visible in the right panel where the differential conductance is plotted as a function of the generalized order of the MAR process $m' = 2\Delta/eV$. For small T the onset of the MAR processes is equidistant with spacing $2\Delta/eV$ and their amplitudes decrease very rapidly with m'. For high transmission the position of the maxima is progressively shifted to higher m' values, while the minima correspond approximately to integer values of m'. The experimental data of Fig. 3 display a mixed character of high T and low T behavior, because of the presence of the two extreme channels with $T_1 = 0.90$ and $T_2 = 0.108$. The value of the temperature dependent gap $\Delta(\Theta)$ can be determined by the peak of the $m = 1$ process, while the rest of the $\mathrm{d}I/\mathrm{d}V$ is dominated by the widely open channel T_1. In the left inset of Fig. 3 we plot the position of the $m = 1$ maximum as a function of the temperature. Also shown are data taken on different contact configurations of the same sample. The development of the peak position follows the BCS gap function $\Delta_{\mathrm{BCS}}(\Theta)$ which is plotted as a solid line in the same graph. We have verified for contacts with different conductances ranging from the tunnel regime to several G_0 that the IVs can be described by the same channel distribution (with restricted accuracy due to less pronounced MAR features) up to the critical temperature. When exceeding Θ_{c} the IV characteristics become linear with a slope corresponding to D within 1%.

VI. IVS OF AL POINT CONTACTS WITH EXTERNAL MAGNETIC FIELD

Fig. 5 shows the evolution of the subgap structure with applied magnetic field. The traces are offset for clarity. In our experiment the field is applied perpendicular to the film plane. As the field size is increased, the excess current is suppressed, the current steps are strongly rounded and the peak positions are shifted to lower voltages. For fields larger than $\approx 5.0\,\mathrm{mT}$ no clear sub-multiple current steps are observable. When a field of $\mu_0 H_{\mathrm{c}} = 10.2\,\mathrm{mT}$ close to the bulk critical field of Al $\mu_0 H_{\mathrm{c,bulk}} = 9.9\,\mathrm{mT}$ is reached the IV becomes again linear with a slope corresponding to the sum D of the transmissions determined in zero field. When lowering the field again to $H = 0$ we recover the same subgap structure as before. When reversing the field direction the same IV is observed for the same absolute value of the field, which proves that there is no residual field along the field axis. Effects of the earth magnetic field or spurious fields in different directions however cannot be excluded.

An external magnetic field suppresses superconductivity because it acts as an effective pair breaking mechanism [32]. Since a magnetic field breaks the electron-hole symmetry, the IVs due to MAR are modified as demonstrated by Zaitsev and Averin [33]. Strictly speaking, the conduction channels could be different with and without magnetic field.

A quantitative description of the influence of the magnetic field is difficult because of the complicated shape of

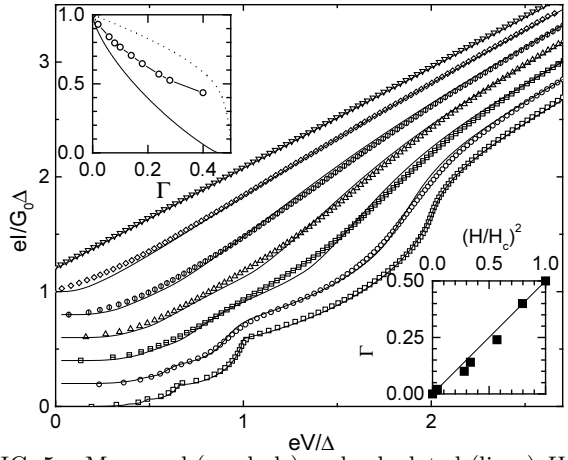

FIG. 5. Measured (symbols) and calculated (lines) IVs of trace (d) of Fig. 1 with transmission set $\{0.519, 0.253, 0.106\}$ for magnetic fields of $\mu_0 H$ = 0, 2.1, 5.4, 5.9, 7.7, 9.1 and 10.9 mT (from bottom to top). The curves with magnetic field are offset by 0.2 each. Left inset: pair amplitude Δ (dotted), spectral gap Ω (solid) (according to [34]) and position of the $m = 1$ maximum of the corresponding calculated dI/dVs (symbols) in units of the gap parameter at zero field as a function of the pair breaking parameter Γ. Right inset: Pair breaking parameter Γ used for calculating the IVs and dI/dVs as a function of applied field (symbols) and prediction according to [32,34] (line). The IV at $H = 0$ was measured at the beginning and the end of the series of measurements and the $\{T_n\}$ was found to be reproducible. The critical field at the measuring temperature of $\Theta = 25$ mK was determined to be $\mu_0 H_c = 10.2$ mT.

the samples. The point contact spectra are sensitive to the superconducting properties at the constriction. Since the pair breaking parameter $\Gamma = \hbar/(2\tau_{pb}\Delta)$ (τ_{pb} is the pair-breaking time) due to an external magnetic field is geometry dependent [32] a complete description needs to take into account the exact shape of the sample on the length scale of the coherence length ξ. We estimate for our Al films in the dirty limit $\xi = (\hbar D_{el}/2\Delta)^{1/2} =$ 280 nm where $D_{el} = v_F l/3 = 0.042$ m^2/s is the electronic diffusion constant.

Due to the finite elastic mean free path $l \approx 65$ nm (determined by the residual resistivity ratio RRR = $R(300\,\mathrm{K})/R(4.2\,\mathrm{K}) \approx 4$) of the evaporated thin film the penetration depth is enhanced and it is comparable to the sample thickness. The fact that all signature of superconductivity is destroyed at the bulk critical field indicates that the geometry of the sample does not play a dominant role, but that ξ is the most important length scale. We therefore describe the influence of the magnetic field along the lines of Skalski *et al.* [34] using a homogeneous Γ given by the expression [32,35]

$$\Gamma = \frac{D_{el} e^2 \mu_0^2 H^2 w^2}{6\hbar\Delta} \qquad (2)$$

where the effective width of the film $w = 280$ nm $\simeq \xi$ is limited by the coherence length. Superconductivity is completely suppressed when $\Gamma = 0.5$. In order to obtain the IV curves for one channel in an external magnetic field, the BCS density of states in the theory of Ref. [10] is replaced by the corresponding expressions given in Refs. [32,34] which include the effect of a pair breaking mechanism.

Contrary to the influence of higher temperatures, the magnetic field rounds the density of states and the Andreev reflection amplitude. The rounding is a consequence of the fact that the pair amplitude Δ and the spectral gap Ω of the density of states (i.e. the energy up to which the density of states is zero) differ from each other when time reversal symmetry is lifted. The position of the $m = 1$ maximum of the dI/dV does not give an accurate estimation of Γ and it is necessary to fit the whole IV. In the left inset we display the evolution (as a function of Γ) of Δ, Ω and the position of the maximum conductance of the $m = 1$ process of the contact whose IVs are shown in Fig. 5. The functional dependence of the latter is not universal but depends on the distribution of transmissions.

It turns out that the structure in the experimental data is more rounded than in the calculated curves indicating the limitations of the model used here. A reasonable agreement between the experimental data and the model is found when determining Γ such that the excess current is correctly described. The solid lines in Fig. 5 are calculated with the transmission ensemble determined at zero field for values of Γ given in the inset. These values correspond nicely to the predicted quadratic behavior of

Eq. 2. It was not possible to achieve better agreement between the measured and calculated IVs by altering the channel ensemble, supporting again that the conduction channels are not affected by superconductivity, nor by its suppression [36].

We have demonstrated here, that it is possible to drive a particular contact reproducibly into the normal state and back to the superconducting state without changing $\{T_n\}$. We stress the high stability of the setup necessary for maintaining a particular contact stable during the measurement series.

VII. CONCLUSIONS

We have reported measurements and the analysis of multiple Andreev reflection in superconducting atomic contacts demonstrating that the conduction channel ensemble of the smallest point contacts between Al electrodes consists of at least two, more often three channels. We have verified that the channel ensemble remains unchanged when suppressing the superconductivity gradually by increasing the temperature or applying a magnetic field. This result strongly supports the expected equivalence of conduction channels in the normal and in the superconducting state and agrees with the quantum chemical picture of conduction channels. The latter suggests that the conduction channels are determined by the band structure of the metal and therefore their transmissions vary significantly only on the scale of several eV. Superconductivity, which opens a spectral gap for quasiparticles of the order of only $\simeq$ meV does not modify the channels and is therefore a useful tool to study them.

We thank C. Strunk and W. Belzig for valuable discussions. This work was supported in part by the Deutsche Forschungsgemeinschaft (DFG), Bureau National de Métrologie (BNM), and the Spanish CICYT.

[1] J.M. van Ruitenbeek, in "Mesoscopic Electron Transport", L.L. Sohn, L.P. Kouwenhoven, and G. Schön eds., Amsterdam, 1997, and references therein.
[2] R. Landauer, IBM J. Res. Dev. 1 (1957) 223; Philos. M. 21 (1970) 863.
[3] L. Olesen *et al.*, Phys. Rev. Lett. 72 (1994) 2251.
[4] J.M. Krans *et al.*, Nature 375 (1995) 767.
[5] J.L. Costa-Krämer, N.P. García-Mochales, and P.A. Serena, Surface Science 342 (1995) L1144.
[6] A.I. Yanson and J.M. van Ruitenbeek, Phys. Rev. Lett. 79 (1997) 2157.
[7] E. Scheer *et al.*, Phys. Rev. Lett. 78 (1997) 3535.
[8] L.B. Arnold, Journal of Low Temp. Phys. 68 (1987) 1.
[9] D. Averin and A. Bardas, Phys. Rev. Lett. 75 (1995) 1831.
[10] J.C. Cuevas, A. Levy Yeyati, and A. Martín-Rodero, Phys. Rev. B 54 (1996) 7366.
[11] E.N. Bratus *et al.*, Phys. Rev. B 55 (1997) 12666.
[12] The four works [8–11] deal through different approaches with the same physics and provide essentially the same results for the IV. We have used the numerical results provided by [10] in order to draw the inset of Fig. 1 and to perform the fits.
[13] J.C. Cuevas, A. Levy Yeyati, A. Martín-Rodero, Phys. Rev. Lett. 80 (1998) 1066.
[14] E. Scheer *et al.*, Nature 394 (1998) 154.
[15] E. Scheer, W. Belzig, Y. Naveh, D. Esteve, C. Urbina, and M.H. Devoret, in preparation.
[16] H.E. van den Brom, J.M. van Ruitenbeek, Phys. Rev. Lett. 82 (1999) 1526
[17] B. Ludoph *et al.*, Phys. Rev. Lett. 82 (1999) 1530.
[18] B. Ludoph, J.M. van Ruitenbeek, Phys. Rev. B 59 (1999) 12290.
[19] J. Bardeen, L.N. Cooper, and J.R. Schrieffer, Phys. Rev. 108 (1957) 1175.
[20] C.W.J. Beenakker, Phys. Rev. B 46 (1992) 12841.
[21] A. Bardas and D.V. Averin, Phys. Rev. B 56 (1997) R8518.
[22] A. Martin-Rodero, A. Levy Yeyati, J.C. Cuevas, Superlattices and Microstructures, 25 (1999) 925.
[23] J.C. Cuevas, unpublished.
[24] T.M. Klapwijk, G.E. Blonder and M. Tinkham, Physica 109&110B (1982) 1657.
[25] M. Hurd, S. Datta, and P.F. Bagwell, Phys. Rev. B 54 (1996) 6557.
[26] B.N. Taylor and E. Burstein, Phys. Rev. Lett. 10 (1963) 14.
[27] K. Flensberg, and J. Bindslev Hansen, Phys. Rev B 40 (1989) 8693.
[28] A.W. Kleinsasser *et al.*, Phys. Rev. Lett. 72 (1994) 1738.
[29] J.M. van Ruitenbeek *et al.*, Rev. Sci. Inst. 67 (1996) 108.
[30] D.C. Glattli *et al.*, J. Appl. Phys. 81 (1997) 7350.
[31] D. Vion *et al.*, J. Appl. Phys. 77 (1995) 2519.
[32] K. Maki in "Superconductivity", vol. 2, R.D. Parks ed., M. Dekker (New York,1969).
[33] A.V. Zaitsev and D.V. Averin, Phys. Rev. Lett. 80 (1998) 3602.
[34] S. Skalski, O. Betbeder-Matibet, and P.R. Weiss, Phys. Rev. 136 (1964) A1500.
[35] W. Belzig, C. Bruder, and G. Schön, Phys. Rev. B 54 (1996) 9443.
[36] In a recent work by Suderow *et al.* on long neck contacts of Pb prepared in an STM a strongly enhanced critical field was observed. This was explained by the varying sample width on the length scale of ξ, which enables superconductivity in the long neck although the bulk critical field is exceeded. In Al ξ is much larger than in Pb and therefore this effect appears to be negligible for the present work. However, the observed rounding of the MAR structures in our samples might be due to a similar mechanism. H. Suderow *et al.*, cond-mat/9907236.